Inorg. Chem. **2007**, *46*, 9736–9742

Self-Assembly of a Mn_9 Nanoscopic Mixed-Valent Cluster: Synthesis, Crystal Structure, and Magnetic Behavior

Kartik Chandra Mondal,[†] You Song,[‡] and Partha Sarathi Mukherjee*,[†]

Department of Inorganic and Physical Chemistry, Indian Institute of Science, Bangalore 560012, India, and Coordination Chemistry Institute and the State Key Laboratory of Coordination Chemistry, Nanjing University, Nanjing 210093, China

Received May 25, 2007

A rare Mn_9 μ_3-oxo-centered mixed-valent cluster $[Mn_9O_7(O_2CPh)_{11}(thmn)(py)_2(H_2O)_3]$ (**1**) is prepared by assembling an oxo-centered $Mn^{II}Mn^{III}_2$ triangle, $[Mn_3O(O_2CPh)_6(py)_2(H_2O)]\cdot 0.5MeCN$, as the secondary building unit in the presence of a tripodal alcohol, 1,1,1-tris(hydroxymethyl)nitromethane (H_3thmn), as the capping ligand. Complex **1** was formed along with a minor byproduct, $[Mn_6O_2(O_2CPh)_{10}(MeCN)_4]$ (**2**). Complex **1** was characterized by X-ray single-crystal structure analysis and was crystallized in a monoclinic system, space group $P2_1/n$, $a = 16.214(6)$ Å, $b = 25.874(10)$ Å, $c = 26.497(10)$ Å, and $\beta = 94.214(7)°$. The Manganese–oxo–carboxylate core in **1** looks like a funnel. Variable-temperature magnetic studies down to 2 K reveal the existence of dominant ferromagnetic interaction within the cluster. Alternating current susceptibility data of the cluster show strong frequency dependence of both the real and imaginary parts of susceptibility χ' and χ'' below 5 K. Moreover, the calculated relaxation time, $\tau_0 = 1.2 \times 10^{-7}$ s, and the energy barrier, $\Delta E = 25$ K, are consistent with the single-molecule magnetic behavior of **1**.

Introduction

The field of molecular magnetism has attracted considerable attention, and major advances have been made in their application as novel molecule-based magnets.[1] Recently, special attention has been paid to the design and synthesis of discrete magnetic clusters[2] because paramagnetic clusters with large-spin ground states can display the phenomenon of single-molecule magnetism.[2] Research on single-molecule magnets (SMMs) is a key factor in the search for more efficient ways to store digital information. Whereas currently used extended magnets rely on the collective behavior of

* To whom correspondence should be addressed. E-mail: psm@ipc.iisc.ernet.in. Tel.: 91-80-2293-3352. Fax: 91-80-2360-1552.

† Indian Institute of Science.

‡ Nanjing University.

(1) (a) Miller, J. S.; Epstein, A. J.; Reiff, W. M. *Science* **1988**, *240*, 40. (b) Miller, J. S.; Epstein, A. J.; Reiff, W. M. *Chem. Rev.* **1988**, *88*, 201. (c) Kahn, O.; Pei, Y.; Verdaguer, M.; Renard, J. P.; Sletten, J. *J. Am. Chem. Soc.* **1988**, *110*, 782. (d) Arrio, M. A.; Sculiller, A.; Sainctavit, P.; Moulin, C. D.; Mallah, T.; Verdaguer, M. *J. Am. Chem. Soc*. **1999**, *121*, 6414. (e) Yanai, N.; Kaneko, W.; Yoneda, K.; Ohba, M.; Kitagawa, S. *J. Am. Chem. Soc*. **2007**, *129*, 3496. (f) Kaneko, W.; Kitagawa, S.; Ohba, M. *J. Am. Chem. Soc.* **2007**, *129*, 248. (g) Sessoli, R.; Tsai, H.-L.; Schake, A. R.; Wang, S.; Vincent, J. B.; Folting, K.; Gatteschi, D.; Christou, G.; Hendrickson, D. N. *J. Am. Chem. Soc*. **1993**, *115*, 1804. (h) Konar, S.; Corbella, M.; Zangrando, E.; Ray Chaudhuri, N. *Chem. Commun.* **2003**, 1424. (i) Ouellette, W.; Galan-Mascaros, J. R.; Dunbar, K. R.; Jubieta, J. *Inorg. Chem*. **2006**, *45*, 1909. (j) Shatruk, M.; Dragulescu, A. A.; Chambers, K. E.; Stoian, S. A.; Bominaar, F. A.; Achim, C.; Dunbar, K. R. *J. Am. Chem. Soc*. **2007**, *129*, 6104. (k) Konar, S.; Zangrando, E.; Drew, M. G. B.; Mallah, T.; Ribas, J.; Ray Chaudhuri, N. *Inorg. Chem.* **2003**, *42*, 5966. (l) Price, D. J.; Batten, S. R.; Murry, K. S. *Chem. Commun*. **2002**, 762. (m) Chen, P. K.; Che, Y. X.; Batten, S. R. *Chem. Mater*. **2007**, *19*, 2162. (n) Liu, F. C.; Zeng, Y. F.; Jiao, J.; Li, J. R.; Bu, X. H.; Ribas, J.; Batten, S. R. *Inorg. Chem*. **2006**, *45*, 6129.

(2) (a) Konar, S.; Bhuvanesh, N.; Clearfield, A. *J. Am. Chem. Soc*. **2006**, *128*, 9604. (b) Mao, J. G.; Clearfield, A. *Inorg. Chem.* **2002**, *41*, 2319. (c) Nehete, U. N.; Anantharaman, G.; Chandrasekhar, V.; Murugavel, R.; Walawalkar, M. G.; Roesky, H. W.; Vidovic, D.; Magull, J.; Samwer, K.; Sass, B. *Angew. Chem., Int. Ed.* **2004**, *43*, 3832. (d) Nehete, U. N.; Chandrasekhar, V.; Anantharaman, G.; Roesky, H. W.; Vidovic, D.; Magul, J. *Angew. Chem., Int. Ed.* **2004**, *43*, 3842. (e) Winpenny, R. E. P. *Dalton Trans.* **2002**, 1. (f) Brechin, E. K. *Chem. Commun*. **2005**, 5141. (g) Parsons, S.; Christou, G. *Chem. Commun.* **2002**, 2252. (h) Brechin, E. K.; Soler, M.; Christou, G.; Davidson, J.; Hendrickson, D. N.; Parsons, S.; Wernsdorfer, W. *Polyhedron* **2003**, *22*, 1771. (i) Piligkos, S.; Rajaraman, G.; Soler, M.; Kirchner, N.; Slageren, J.; Bircher, R.; Parsons, S.; Güdel, H. U.; Kortus, J.; Wernsdorfer, W.; Christou, G.; Brechin, E. K. *J. Am. Chem. Soc.* **2005**, *127*, 5572. (j) Pan, S.; Watkins, B.; Smit, J. P.; Marvekl, M. R.; Saratovsky, I.; Poeppelmeier, K. R. *Inorg. Chem.* **2007**, *46*, 3851. (k) Sessoli, R.; Gatteschi, D.; Caneschi, A.; Novak, M. A. *Nature* **1993**, *365*, 141. (l) Ruiz, D.; Sun, Z.; Albela, B.; Folting, K.; Ribas, J.; Christou, G.; Hendrickson, D. N. *Angew. Chem., Int. Ed.* **1998**, *37*, 300. (m) Tasiopoulos, A. T.; Vinslava, A.; Wernsdorfer, W.; Abboud, K. A.; Christou, G. *Angew. Chem., Int. Ed.* **2004**, *43*, 2117. (n) Wernsdorfer, W.; Aliaga-Alcalde, N.; Hendrickson, D. N.; Christou, G. *Nature* **2002**, *416*, 406. (o) Ako, A. M.; Hewitt, I. J.; Mereacre, V.; Clérac, R.; Wernsdorfer, W.; Anson, C. E.; Powell, A. K. *Angew. Chem., Int. Ed.* **2006**, *45*, 4926. (p) Milios, C. J.; Fabbiani, F. P. A.; Parsons, S.; Murugesu, M.; Christou, G.; Brechin, E. K. *Dalton Trans.* **2006**, 351.

10.1021/ic701018x CCC: $37.00
Published on Web 10/05/2007

the unpaired spins of several millions of metal ions present in a certain amount of the material, with SMMs, each individual molecule acts as a very small magnet that can be used to store information. The much smaller size of SMMs compared with traditional magnets means more information can be stored on hard drives and other devices, with obvious huge commercial and industrial benefits. Major works on SMMs have been done on the Mn_{12}-acetate cluster and its derivatives, with recent developments on polyhydroxy-bridged SMMs by Brechin, Christou, and others.[2] Two distinct approaches to the synthesis of polynuclear metal complexes are as follows: designed assembly,[1b−d] in which the use of rigid ligands with a directional bonding approach leads to predesigned structures, and "serendipitous" assembly,[2] in which the ligands are more flexible and the resulting structures are not predictable. In designed self-assembly, it is easy to control the progress of the reaction as well as the shapes of the final products. A danger point of the designed self-assembly approach is that it relies on a limited range of experience and on the imagination of the scientists involved. If ligands are used only where the chemists are confident of the ligands' behavior, the results will be restricted to a limited number of products. In the case of serendipitous assembly, the element of strict design is absent. In contrast to designed assembly, ligands that display several different coordination modes, combined with metal centers that can vary their coordination geometries, are used. Polyhydroxy compounds have proven to be suitable linkers in serendipitous assembly of a variety of polynuclear clusters. Christou, Brechin, and their co-workers have recently developed the method of coupling smaller clusters into larger arrays using several linkers including polyhydroxy ligands.[2] It is also established from some recent results that a simple change in the starting cluster/reaction condition can change the nuclearity as well as the properties of the final clusters drastically. We are working on the self-assembly of polyclusters from the smaller clusters using several supramolecular linkers.[3] Hence, it was of our interest whether a simple change in the bridging trihydroxy ligand has any effect on the nuclearity or properties of the final cluster. We herein introduce 1,1,1-tris(hydroxymethyl)nitromethane (abbreviated as H_3thmn) as the supramolecular linker to grow an oxo-centered Mn_3 triangle to a Mn_9 mixed-valent nanoscopic funnel-type cluster, $[Mn_9O_7(O_2CPh)_{11}(thmn)(py)_2(H_2O)_3]$ (**1**), which shows strong frequency-dependent out-of-phase (χ_M'') signals in alternating current (ac) magnetic measurements.

Experimental Section

Materials. 1,1,1-Tris(hydroxymethyl)nitroethane (H_3thmn) was purchased from Aldrich and used without further purification. The starting oxo-centered neutral triangle $[Mn_3O(O_2CPh)_6(py)_2(H_2O)]\cdot 0.5MeCN$ was prepared according to the published procedure.[4] All solvents were commercially available and were used as received.

Table 1. Crystal Data and Structure Refinement for **1**

compound	**1**
empirical formula	$C_{91}H_{73}N_3O_{37}Mn_9$
fw	2294.98
T/K	100(2)
cryst syst	monoclinic
space group	$P2_1/n$
a/Å	16.214(6)
b/Å	25.874(10)
c/Å	26.497(10)
α/deg	90.00
β/deg	94.214(7)
γ/deg	90.00
V/Å^3	11087 (7)
Z	4
μ(Mo Kα)/mm^{-1}	1.66
λ/Å	0.710 73
R_w[a]	0.2504
R[a]	0.1072
D/Mg m^{-3}	1.521

[a] $R = \sum||F_o| - |F_c||/\sum|F_o|$; $R_w = [\sum\{w(F_o^2 - F_c^2)^2\}/\sum\{w(F_o^2)^2\}]^{1/2}$.

Physical Measurements. Elemental analyses of C, H, and N were performed using a Perkin-Elmer 240C elemental analyzer. IR spectra as KBr pellets were recorded on a Magna 750 FT-IR spectrophotometer. The measurements of variable-temperature magnetic susceptibility and field dependence of magnetization were carried out on a microcrystalline sample of **1** using a Quantum Design MPMS-XL5 SQUID magnetometer. The experimental susceptibilities were corrected for diamagnetism (Pascal's tables).[5]

Preparation of Complex 1. A mixture of H_3thmn (1 mmol, 151 mg) and the neutral triangle $[Mn_3O(O_2CPh)_6(py)_2(H_2O)]\cdot 0.5MeCN$ (0.5 mmol, 551 mg) in MeCN was stirred for 48 h to yield a brown/black solution along with a small amount of precipitate. Removal of the precipitate and subsequent slow diffusion of ether into the brown/black filtrate yielded a dark black/brown plate-shaped crystal of $[Mn_9O_7(O_2CPh)_{11}(thmn)(py)_2(H_2O)_3]$ (**1**). Removal of **1** followed by slow evaporation of the remaining red solution yielded a known Mn_6 cluster, $[Mn_6O_2(O_2CPh)_{10}(MeCN)_4]$ (**2**), as the minor byproduct. Complex **1**. Yield: 35%. IR (KBr): ν 1026, 1648, 1580, 2933, 2859, 1726, 1249, 820 cm^{-1}. Elem anal. Calcd (%) for $C_{91}H_{77}Mn_9N_3O_{37}$: C, 47.51; H, 3.35; N, 1.83. Found: C, 47.80; H, 3.66; N, 1.61. Complex **2**. Yield: 7%. IR (KBr): ν 1652, 1573, 2940 cm^{-1}. Elem anal. Calcd (%) for $C_{78}H_{62}Mn_6N_4O_{22}$: C, 53.91; H, 3.49; N, 3.23. Found: C, 53.70; H, 3.61; N, 3.51.

Crystal Structure Determinations. The single-crystal data were collected using a Bruker SMART APEX CCD diffractometer, equipped with a fine-focus sealed-tube Mo Kα X-ray source. *SMART* was used for data acquisition, and *SAINT* was used for data extraction. The crystals were positioned at 50 mm from the CCD. A total of 321 frames were measured with a counting time of 10 s. Data analysis was carried out with the *Crysalis* program. The structure was solved using direct methods with the *Shelx97* program.[6] The non-hydrogen atoms were refined with anisotropic thermal parameters. The disordered atoms were refined with constrained dimensions. The hydrogen atoms bonded to carbon were included in geometric positions and given thermal parameters equivalent to 1.2 times those of the atom to which they were attached. An absorption correction was carried out using the *ABSPACK* program. The structure was refined on F^2 using *Shelx97*. The crystal structure refinement parameters are given in Table 1.

(3) Mondal, K.; Drew, M. G. B.; Mukherjee, P. S. *Inorg. Chem.* **2007**, *46*, 5625.
(4) Vincent, J. B.; Chang, H. R.; Folting, K.; Huffman, J. C.; Christou, G.; Hendrickson, D. N. *J. Am. Chem. Soc.* **1987**, *109*, 5703.
(5) Kahn, O. *Molecular Magnetism*; VCH Publishers: Berlin, 1993.
(6) Sheldrick, G. M. *SHELXL*; University of Gottingen: Gottingen, Germany, 1997.

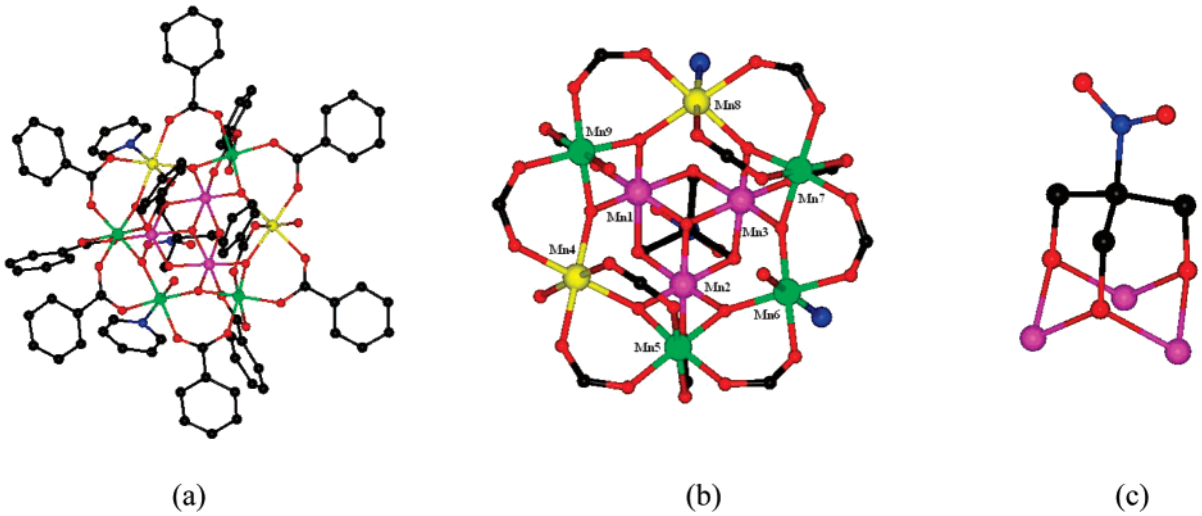

Figure 1. (a) Full view of the molecular structure of **1**, (b) core view, and (c) the bridging mode of thmn^{3-}. Pink balls indicate Mn^{IV} ions of the smaller triangular ring. Green and yellow balls represent the Mn^{III} and Mn^{II} ions of the hexagonal ring, respectively. Black balls represent the carboxylate carbons of the benzoates.

Results and Discussion

Synthesis. The reaction of the H_3thmn ligand with 0.5 equiv of an oxo-centered triangle, $[Mn_3O(O_2CPh)_6(py)_2(H_2O)]\cdot 0.5MeCN$, in MeCN produced a black/brown solution. Slow diffusion of ether into this solution yielded dark-brown **1** in 35% isolated yield in 1 week. The formation of several byproducts in the preparation of manganese clusters is a common fact. Complex **1** contains two Mn^{2+}, four Mn^{3+}, and three Mn^{4+} ions and is prepared from a $Mn^{II}Mn^{III}_2$ cluster, meaning that its formation is a complicated mechanism involving deprotonation of the ligand, structural rearrangements, and redox chemistry of many species present in the solution. In fact, complex **1** was also produced along with a byproduct. Because of less solubility, **1** was crystallized first and the remaining light-red solution gave a known $Mn^{II}_4Mn^{III}_2$ cluster, **2**, containing no thmn^{3-} ligand. Single-crystal structure determination and elemental analysis established the composition and the structure of **2**. When the same triangle $[Mn_3O(O_2CPh)_6(py)_2(H_2O)]\cdot 0.5MeCN$ was treated with 1,1,1-tris(hydroxymethyl)ethane, the dodecanuclear rodlike complex $[Mn_{12}O_4(OH)_2(O_2CPh)_{12}(thme)_4(py)_2]$ was formed, which was characterized earlier by the Christou group.[7] Thus, a simple substitution of the so-called inert methyl group in the 1,1,1-tris(hydroxymethyl)ethane by a nitro group has yielded a product of completely different nuclearity, structure, and magnetic behavior. To the best of our knowledge, only a single example is known of this kind of structure containing an acetate ligand and a different trihydroxy linker.[2i] It is interesting to note that, in almost all of the trihydoxy ligands used in the construction of manganese clusters, electron-pushing alkyl groups are present (either methyl or ethyl).[2p] This prompted us to use a trihydroxy ligand containing electron-withdrawing groups like nitro because this electron-pulling effect could enhance the deprotonation of the O−H groups to make the trihydroxy ligand more reactive even in the absence of an external base. The proposed redox equation for the above transformation is as follows:

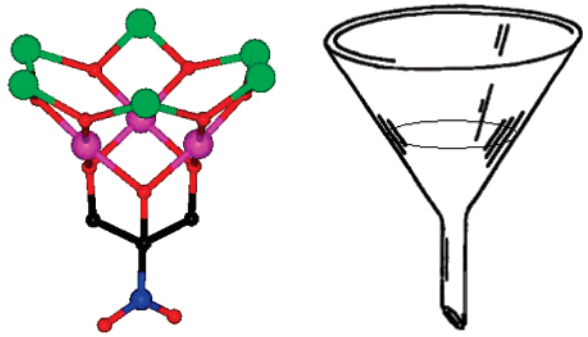

Figure 2. Manganese oxide core of cluster **1** (left), which is compared with a funnel (right).

$$3Mn^{III}_2Mn^{II} - 4e^- \rightarrow Mn^{IV}_3Mn^{III}_4Mn^{II}_2$$

$$3Mn^{III}_2Mn^{II} + 4e^- \rightarrow 2Mn^{III}_2Mn^{II}_4$$

$$3Mn^{III}_2Mn^{II} + 3Mn^{III}_2Mn^{II} \rightarrow Mn^{IV}_3Mn^{III}_4Mn^{II}_2 + 2Mn^{III}_2Mn^{II}_4$$

Crystal Structure of 1. The dark crystals are highly solvent-dependent and become unsuitable for X-ray diffraction in a few seconds if taken out of the mother liquor, while that of **2** are stable in ambient temperature. X-ray crystal structure determination of **1** revealed the formation of a funnel-type Mn_9 cluster, where all of the manganese ions are in distorted octahedral geometries (Figure 1). The funnel consists of a $[Mn_3O]$ oxo-centered triangle, which is sitting on a $[Mn_6O_6]$ hexagon (Figure 2). The smaller ring is capped on one side by the μ_6-trihydroxy ligand, which is functioning

(7) (a) Brechin, E. K.; Soler, M.; Christou, G.; Helliwell, M.; Teat, S. G.; Wernsdorfer, W. *Chem. Commun.* **2003**, 1276. (b) Rajaraman, G.; Murugesu, M.; Soler, M.; Helliwell, M.; Teat, S. G.; Wernsdorfer, W.; Christou, G.; Brechin, E. K. *J. Am. Chem. Soc.* **2004**, *126*, 15445. (c) Koo, B. K.; Lee, U.; *Bull. Korean Chem. Soc.* **2001**, *22*, 103. (d) Murugesu, M.; Raftery, J.; Wernsdorfer, W.; Christou, G.; Brechin, E. K. *Inorg. Chem.* **2004**, *43*, 4203. (e) Mishra, A.; Wernsdorfer, W.; Parsons, S.; Christou, G.; Brechin, E. K. *Chem. Commun.* **2005**, 2086.

Table 2. Selected Bond Lengths (Å) and Angles (deg) for **1**

Mn1−O6	1.838(7)	Mn1−O5	1.895(7)	Mn1−O1	1.925(7)
Mn1−O3	1.939(7)	Mn1−O10	1.955(8)	Mn1−O12	1.808(7)
Mn2−O5	1.903(11)	Mn2−O4	1.931(8)	Mn2−O3	1.946(7)
Mn2−O11	1.805(7)	Mn2−O8	1.953(7)	Mn2−O19	1.843(7)
Mn3−O1	1.990(7)	Mn3−O5	1.907(7)	Mn3−O7	1.915(6)
Mn3−O8	1.994(7)	Mn3−O16	1.809(13)	Mn3−O2	1.791(7)
Mn4−O11	2.122(7)	Mn4−O16	2.120(8)	Mn4−O30	2.155(10)
Mn4−O34	2.143(10)	Mn4−O26	2.180(10)	Mn4−N3	2.197(13)
Mn5−O11	1.873(7)	Mn5−O31	1.971(8)	Mn5−O19	1.903(8)
Mn5−O29	1.931(10)	Mn5−O25	2.238(10)	Mn5−O32	2.171(12)
Mn6−O6	1.927(8)	Mn6−O24	1.992(9)	Mn6−O19	1.914(8)
Mn6−O21	1.991(8)	Mn6−O27	2.207(9)	Mn6−N2	2.234(10)
Mn7−O33	1.974(9)	Mn7−O12	1.867(7)	Mn7−O9	1.943(8)
Mn7−O6	1.907(7)	Mn7−O20	2.244(11)	Mn7−O28	2.172(10)
Mn8−O22	2.151(9)	Mn8−O2	2.136(7)	Mn8−O37	2.299(11)
Mn8−O17	1.197(9)	Mn8−O12	2.124(7)	Mn8−O18	2.132(8)
Mn9−O23	2.199(9)	Mn9−O14	2.269(8)	Mn9−O15	1.966(8)
Mn9−O16	1.884(8)	Mn9−O13	1.982(9)	Mn9−O2	1.895(8)
O12−Mn1−O6	85.2(3)	O3−Mn2−O8	89.5(3)	O12−Mn1−O3	176.3(3)
O6−Mn1−Mn5	93.1(3)	O7−Mn3−O5	163.8(3)	O5−Mn2−Mn4	168.5(3)
O12−Mn1−O1	93.9(3)	O12−Mn1−O5	96.9(3)	O2−Mn3−O5	95.5(3)
O11−Mn2−O19	84.89(3)	O6−Mn1−O1	174.3(3)	O2−Mn3−O5	93.5(3)

as the tail of the funnel. The average Mn−O−Mn bond angle formed by the alkoxy oxygens of the trihydroxy ligand and three Mn^{IV} ions of the triangular ring is 96.4°, while the average of the Mn−O−Mn bond angles formed by the μ_3-oxo and three Mn^{IV} ions is 100°. Both of these bond angles fall in the range to mediate ferromagnetic interaction. The manganese ions of the smaller ring are assumed to be Mn^{IV}, while the hexagonal ring is composed of four Mn^{III} and two Mn^{II} ions. The identity of the oxidation states of the manganese ions was established from the bond-valence calculations as well as the bond parameters (Table 2).

The smaller triangular ring is connected to the hexagonal ring via six μ_3-oxides and three bridging benzoates. The remaining eight benzoates bridge the manganese ions in the hexagonal ring (Figure 1a). Each of the three manganese ions of the hexagonal ring is coordinated to one water molecule. The oxidation states of the manganese ions are assigned based on the total charge balance, bond lengths, and bond-valence calculations. Expected Jahn−Teller elongations of the Mn^{III} ions were observed. The average bond length of Mn^{IV}−O bonds is 1.89 Å, while those for Mn^{II}−O/N and Mn^{III}−O/N are 2.1 and 1.96 Å, respectively. The diameter of the funnel measured by the distance between the opposite carboxylate carbons in the hexagonal ring is 10.75 Å. Structural analysis of complex **2** showed the formation of a Mn_6 cluster, the core of which is identical with the mixed-valent cluster reported earlier.[8c]

The bond-valence calculations of complex **1** and selected bond parameters are assembled in Tables 2 and 3, respectively. Strong hydrogen-bonding interactions among the coordinated water molecules and carboxylate oxygens were found within the individual cluster. However, no intercluster hydrogen bonding was found in the solid-state structure. A packing diagram (Figure 3) reveals the presence of intercluster $\pi-\pi$ supramolecular interaction between the phenyl rings of the neighboring clusters in the solid state of **1**.

The crystal quality of cluster **2** was not good. However, a data set at room temperature showed the exact connectivity and composition of **2** for this complex. This structure consists of six manganese atoms arranged as two edge-sharing tetrahedra (Figure 4). This structure can be considered as if two "oxo-centered beryllium acetate type" tetrahedra are joined through a common edge. The geometry around each manganese is distorted octahedral with six oxygen atoms around each metal center. The center of each tetrahedron is occupied by a μ_4-O^{2-} ion. Each nonsharing manganese is coordinated to one MeCN molecule; other coordination sites of each manganese are satisfied by bridging carboxylates. The cluster is neutral and the total negative charge due to 10 carboxylates and 2 oxo anions is 14. Therefore, charge consideration and bond parameters indicate a mixed-valent $Mn^{III}_2Mn^{II}_4$-type composition. This mixed-valent cluster contains two tetrahedral O^{2-} and is identical with a known cluster reported earlier.[8c] The only difference is the presence of two coordinated MeCN molecules.

Magnetic Behavior. Solid-state variable-temperature magnetic susceptibility data were measured in the temperature range of 300−2 K in an applied magnetic field of 200 G. $\chi_M T$(300 K) = 16.62 emu K mol^{-1} is much lower than the spin-only value of 26.375 emu K mol^{-1} based on the $Mn^{II}_2Mn^{III}_4Mn^{IV}_3$ unit. A minimum of 16.07 emu K mol^{-1} at 250 K and a maximum of 37.9 emu K mol^{-1} at 14 K were observed (Figure 5). This plot shows a ferrimagnetic-like behavior, indicating the coexistence of both antiferro- and ferromagnetic coupling between manganese ions in this cluster. The antiferromagnetic interaction in the low-temperature region may also be due to the weak intercluster supramolecular $\pi-\pi$ interaction through the phenyl rings of the neighboring molecule, as is evident from the packing diagram (Figure 3). The maximum is slightly lower than the value of 40.37 emu K mol^{-1} based on $S_T = {}^{17}/_2$ and assuming $g = 2$. Some attempts have been done for fitting the magnetic

(8) (a) Tsukerblat, B. S. *Inorg. Chem.* **1999**, *38*, 6081. (b) Borrás-Almenar, J. J.; Clemente-Juan, J. M.; Coronado, E.; Tsukerblat, B. S. *J. Comput. Chem.* **2001**, *22*, 985. (c) Schake, A. R.; Vincent, J. B.; Li, Q.; Boyd, P. D. W.; Folting, K.; Huffman, J. C.; Christou, G. *Inorg. Chem.* **1989**, *28*, 1915.

Table 3. Bond-Valence Calculations for Cluster **1**

A_i	B_j	bond (r_{ij}) length (Å)	S_{ij}	ΣS_{ij}	conclusion
Mn1	O5	1.895	0.681		
Mn1	O10	1.955	0.579		
Mn1	O12	1.808	0.861	4.143	Mn^{IV}
Mn1	O1	1.925	0.628		
Mn1	O6	1.839	0.792		
Mn1	O3	1.939	0.604		
Mn2	O5	1.903	0.666		
Mn2	O4	1.931	0.618		
Mn2	O3	1.946	0.593	4.111	Mn^{IV}
Mn2	O11	1.805	0.868		
Mn2	O8	1.953	0.582		
Mn2	O19	1.843	0.784		
Mn3	O5	1.907	0.595		
Mn3	O7	1.915	0.645		
Mn3	O8	1.994	0.521	4.049	Mn^{IV}
Mn3	O2	1.791	0.902		
Mn3	O1	1.990	0.527		
Mn3	O16	1.809	0.859		
Mn4	O11	2.122	0.407		
Mn4	O16	2.120	0.409		
Mn4	O30	2.155	0.372	2.322	Mn^{II}
Mn4	O34	2.143	0.385		
Mn4	O26	2.180	0.348		
Mn4	N3	2.197	0.404		
Mn5	O11	1.873	0.736		
Mn5	O31	1.971	0.565		
Mn5	O19	1.903	0.679	3.212	Mn^{III}
Mn5	O29	1.931	0.629		
Mn5	O25	2.238	0.274		
Mn5	O32	2.171	0.329		
Mn6	O24	1.992	0.534		
Mn6	O19	1.914	0.659		
Mn6	O6	1.927	0.636	3.000	Mn^{III}
Mn6	O21	1.991	0.535		
Mn6	O27	2.207	0.298		
Mn6	N2	2.234	0.337		
Mn7	O33	1.974	0.560		
Mn7	O12	1.867	0.748		
Mn7	O9	1.943	0.609	3.187	Mn^{III}
Mn7	O6	1.907	0.672		
Mn7	O20	2.244	0.270		
Mn7	O28	2.172	0.328		
Mn8	O22	2.151	0.376		
Mn8	O2	2.136	0.392		
Mn8	O37	2.299	0.252	2.153	Mn^{II}
Mn8	O17	2.197	0.332		
Mn8	O12	2.124	0.405		
Mn8	O18	2.132	0.396		
Mn9	O23	2.199	0.305		
Mn9	O14	2.269	0.252		
Mn9	O15	1.966	0.573	3.087	Mn^{III}
Mn9	O16	1.884	0.715		
Mn9	O13	1.982	0.548		
Mn9	O2	1.895	0.694		

properties by the MAGPACK package,[8] but no result was obtained because of too many coupling parameters leading to too many eigenvalues in the highly asymmetrical structure of the cluster. To determine the spin ground state of the cluster magnetization, data were collected in the ranges of 1−7 T and 1.8−10 K, and the reduced magnetization data vs H/T is plotted in Figure 5. The solid lines are the fitting results using ANISOFIT[8] to give $g = 1.94$, $S = {}^{17}/_{2}$, $D = -0.26$ cm^{-1}, and $E = 2 \times 10^{-5}$ cm^{-1}. So, energy barrier $\Delta E = S^2|D| = 18.8$ cm^{-1}. This spin ground state can be achieved by the antiferromagnetic interaction between the ferromagnetically coupled triangular and hexagonal rings in the funnel. No hysteresis loop was found when M vs H data (−5 to +5 T) at 2 K were plotted.

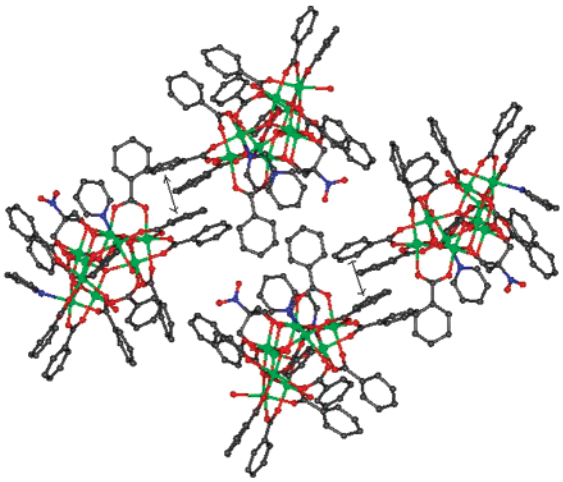

Figure 3. Packing diagram of cluster **1** in the solid state. Arrows represent the $\pi-\pi$ interactions among the phenyl rings.

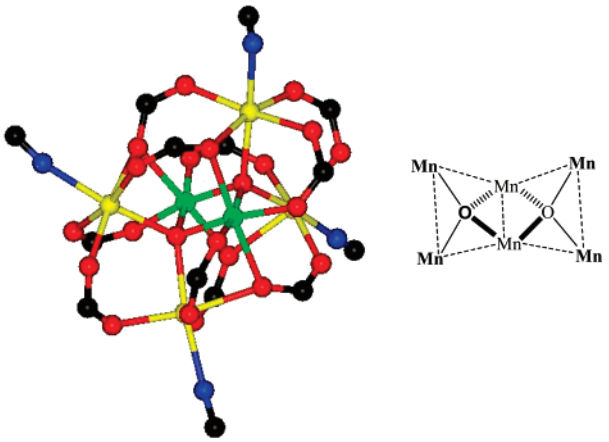

Figure 4. View of the core structure of **2** omitting the phenyl rings for the sake of clarity (left) and representation of the two edge-sharing Mn_4O tetrahedra (right). Green and yellow balls represent Mn^{III} and Mn^{II} ions, respectively.

On the basis of the high ground spin state as well as the nature of D, ac magnetic measurements were preformed to see whether the cluster could function as a SMM. ac susceptibility data of the cluster were measured and showed the strong frequency dependence of both the real and imaginary parts of susceptibility χ' and χ'' below 5 K (Figure 6). Each χ' and χ'' for **1** at a selected frequency goes through a maximum. The maxima shift to high temperature with increasing frequency. This strong frequency dependence of the susceptibilities in ac measurement is a clear characteristic of a SMM.

The T_p's in the plot of χ'' vs T (T_p = peak temperature) educe a linear plot of T_p^{-1} vs $\ln(2\pi\nu)$, which is in good agreement with the Arrhenius law, $1/T_p = -(k_B/\Delta E)[\ln(2\pi\nu) + \ln(\tau_0)]$. The best fit gives the relaxation time $\tau_0 = 1.2 \times$

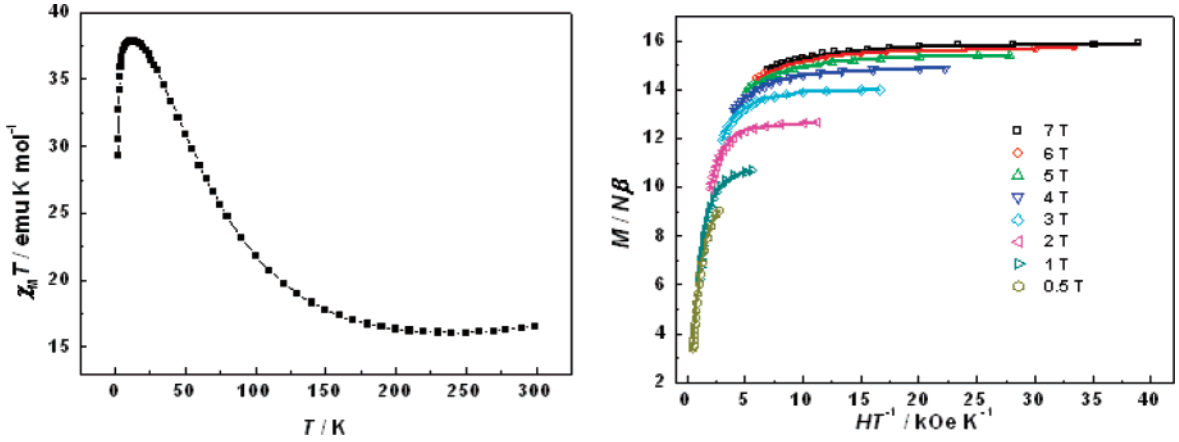

Figure 5. Temperature dependence of magnetic susceptibility in the form of $\chi_M T$ at an applied field of 0.2 kOe. The solid line is a guide for the eyes (left). Plot of reduced magnetization M vs HT^{-1} in the range of 1.8−10 K for this cluster. The solid lines are the fitting results using ANISOFIT[8] (right).

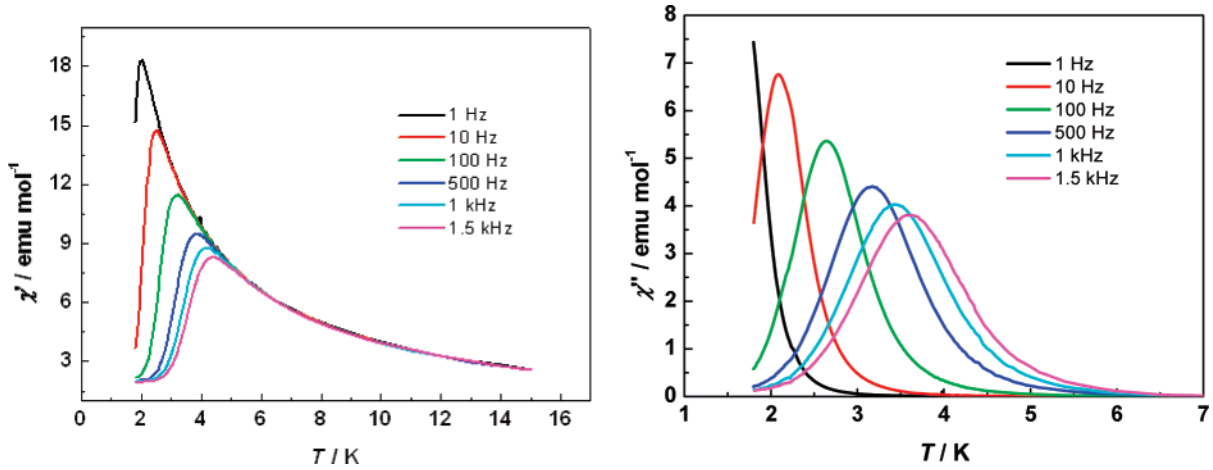

Figure 6. Plots of the in-phase (χ') and out-of-phase (χ'') signal in ac susceptibility vs temperature in an applied field of 4 G at the indicated frequencies.

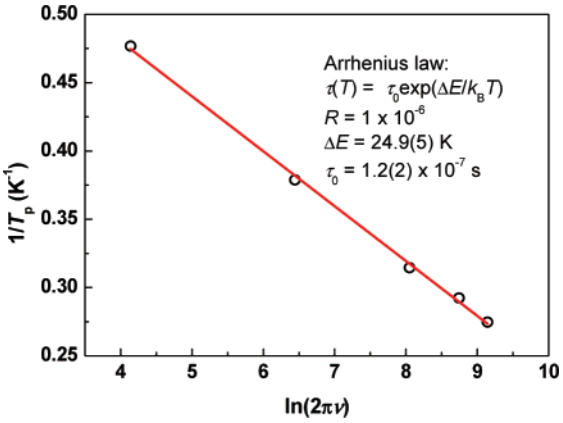

Figure 7. Fitting by the Arrhenius law: $1/T_p = -(k_B/\Delta E)[\ln(2\pi\nu) + \ln(\tau_0)]$. T_p and ν are the peak temperature in $\chi''-T$ and frequency, respectively.

10^{-7} s and the energy barrier $\Delta E = 25$ K, which are also consistent with the SMM behavior (Figure 7).

Complex **1** was obtained from a simple antiferromagnetic oxo-centered triangle $[Mn_3O]^{6+}$. This can be considered as the fused derivative of three such triangles with the assistance of some redox reaction; still **1** potentially shows SMM behavior. Hence, there must be some structural rearrangements that make complex **1** a member of the SMM family. The charge balance and bond-valence-sum calculations suggest that complex **1** consists of one $[Mn^{IV}{}_3O]^{10+}$ in the center of the molecule, which can be considered as a part of a $Mn_4^{IV}O_4$ heterocubane with one of the four Mn^{IV} ions missing and a outer ring of $[Mn_2^{II}Mn_4^{III}O_6]^{4+}$ surrounding the central core. All Mn^{III} ions are distorted because of the Jahn−Teller effect and show bond elongation along the z axis. The central μ_3-O^{2-} in the plane of the Mn_3 triangle mediates the antiferromagnetic coupling via $M_{d\pi}-O_{p\pi}-M_{d\pi}$ orbital overlap in the starting $[Mn_3O(O_2CPh)_6(py)_2(H_2O)]\cdot 0.5MeCN$ complex,[9] while in complex **1**, the central μ_3-O^{2-} (O5) ion is 0.88 Å above the Mn_3^{IV} plane because of capping of μ_6-thmn^{3-} to three Mn^{IV} ions, and hence this O^{2-} (O5) mediates ferromagnetic coupling among the Mn^{IV} ions in the central triangle because of its structural distortion.[10] In complex **1**, all of the $Mn^{IV}-O5-Mn^{IV}$ angles are close to 100° and the angles between two Mn^{IV} ions and an alkoxy oxygen atom (Mn1−O3−Mn2 = 96.05°; Mn2−O8−Mn3 = 96.01°; Mn1−O1−Mn3 = 97.26°) are below 100°. Hence, all of the structural parameters support the ferromagnetic coupling within the central $[Mn^{IV}{}_3O]^{10+}$ triangular unit. The

(9) Jones, L. F.; Rajaraman, G.; Brockman, J.; Murugesu, M.; Sanudo, C. E.; Raftery, J.; Teat, S. J.; Wernsdorfer, W.; Christou, G.; Brechin, E. K.; Collison, D. *Chem.—Eur. J.* **2004**, *10*, 5180.
(10) Stamatatos, T. C.; Albiol, D. F.; Stoumpos, C. C.; Raptopoulou, C. P.; Terzis, A.; Wernsdorfer, W.; Perlepes, S. P.; Christou, G. *J. Am. Chem. Soc.* **2005**, *127*, 15380.

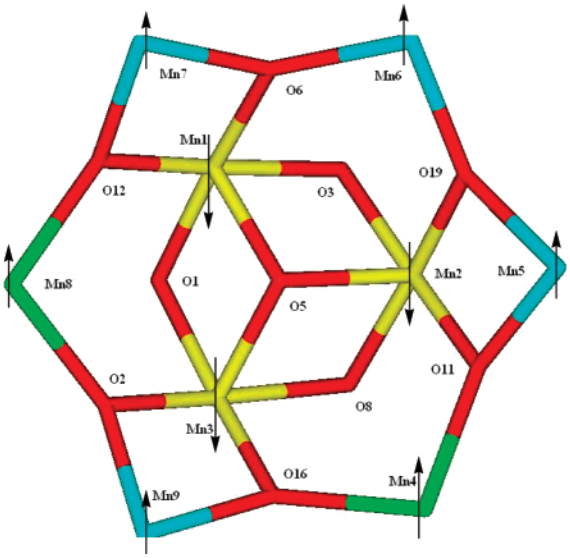

Figure 8. Schematic diagram of the magnetic interactions in complex **1**. Color code: O^{2-}, red; Mn^{II}, green; Mn^{III}, sky blue; Mn^{IV}, yellow. Arrows indicate the spin-up and spin-down.

outer core $[Mn_2^{II}Mn_4^{III}O_6]^{4+}$ is connected to the inner core $[Mn^{IV}{}_3O]^{10+}$ by six μ_3-O^{2-} ions. In the manganese oxide core, Mn1, Mn2, and Mn3 are connected to Mn6, Mn7, and Mn8 ions by μ_3-O6 and μ_3-O12; Mn6, Mn5, and Mn4 ions by μ_3-O19 and μ_3-O11; and Mn4, Mn9, and Mn8 ions by μ_3-O16 and μ_3-O2, respectively, in a triangular fashion. This arrangement is analogous to the Mn_{12}-acetate SMM,[1f] where the $Mn^{IV}{}_4O_4$ heterocubane central core was connected to eight outer Mn^{III} ions in the same fashion. Similarly, in the case of **1**, the ferromagnetically coupled $[Mn^{IV}{}_3O]^{10+}$ triangular unit couples antiferromagnetically with the surrounding four Mn^{III} and two Mn^{II} ions via μ_3-O^{2-} (O6, O19, O11, O16, O2, O12, and O6) bridges to give rise to a total spin of $S = (5 \times 2 + 4 \times 4 - 3 \times 3)/2 = {}^{17}/_2$ (Figure 8).

We think that the SMM behavior of complex **1** is the inescapable consequence of these two antagonist factors, which might have produced the spin frustration[11] in the molecule because of a rare arrangement of the paramagnetic manganese (II, III, or IV) ions in complex **1**.

In conclusion, we have successfully introduced the H_3thmn ligand in the construction of a Mn_9 mixed-valent cluster. The $Mn^{IV}{}_3Mn^{III}{}_4Mn^{II}{}_2$ oxidation state combination of this complex was justified from the charge balance, bond-valence calculations, and magnetic data. Fitting by the Arrhenius law (Figure 7) gives the relaxation time $\tau_0 = 1.2 \times 10^{-7}$ s and the energy barrier $\Delta E = 25$ K, which are consistent with the SMM behavior. Frequency-dependent ac susceptibility data and other parameters clearly demonstrate that the funnel-type Mn_9 cluster **1** is a SMM. While the same starting neutral triangle $[Mn_3O(O_2CPh)_6(py)_2(H_2O)]\cdot 0.5MeCN$ gave a Mn_{12} rod-shaped cluster using 1,1,1-tris(hydroxymethyl)ethane,[7a] a simple substitution of the so-called inert electron-pushing methyl group of the 1,1,1-tris(hydroxymethyl)ethane ligand by an electron-withdrawing nitro group yielded a completely different mixed-valent Mn_9 cluster. So, our present result represents a further example to demand the possibility of linking a magnetically simple smaller cluster by a suitable linker to a larger array with a dramatic change in the magnetic behavior. While most of the studies on SMMs are based on the parent Mn_{12}-acetate cluster and its derivatives, the funnel-type cluster **1** represents an interesting and rare class of SMMs.

Acknowledgment. The authors acknowledge the Department of Science and Technology, New Delhi, Government of India, for financial support to P.S.M. (Fast Track Proposal for Young Scientists).

Supporting Information Available: X-ray crystallographic file in CIF format, structure refinement parameters of **2**, and ZFC-FC/$\chi'T$ vs T plots for **1**. This material is available free of charge via the Internet at http://pubs.acs.org.

IC701018X

(11) (a) McCusker, J. K.; Cheryl, A. C.; Hagen, P. M.; Chadha, R. K.; Harvey, D. F.; Hendrickson, D. N. *J. Am. Chem. Soc.* **1991**, *113*, 6114. (b) McCusker, J. K.; Vincent, J. B.; Schmitt, E. A.; Mino, M. L.; Shin, K.; Coggin, K. D.; Hagen, P. M.; Huffman, J. C.; Christou, G.; Hendrickson, D. N. *J. Am. Chem. Soc.* **1991**, *113*, 3012.